Phase behaviour in a thermotropic polyether involving rod-like mesogenic groups based on conformational isomerism

Stephen Z. D. Cheng* and Michael A. Yandrasits
Institute and Department of Polymer Science, College of Polymer Science and Polymer Engineering, The University of Akron, Akron, Ohio 44325-3909, USA

and Virgil Percec
Department of Macromolecular Science, Case Western Reserve University, Cleveland, Ohio 44106, USA
(Received 26 December 1989; revised 4 May 1990; accepted 17 May 1990)

A thermotropic polyether (MBPE-5) which was synthesized by coupling of 1-(4-hydroxyphenyl)-2-(2-methyl-4-hydroxyphenyl)ethane and α,ω-dibromopentane shows complicated phase transition behaviour. Our thermal analysis, polarized light microscopy and wide angle X-ray diffraction results lead to a recognition of a liquid crystalline phase in this polymer, and it is monotropic. In addition, crystals with two different metastabilities are identified. The more stable crystal grows from its melt in a high isothermal temperature region, characterized by a normal spherulitic texture with banding pattern. The less stable crystal develops from its parent liquid crystalline phase in a low temperature region. The schlieren texture is still kept after this crystallization. Isothermally, in an intermediate temperature region, mixed crystals, formed by both different stabilities, can be observed.

(Keywords: conformational isomerism; crystallization; monotropic; morphology; polyether; rod-like mesogenic group; thermotropic)

INTRODUCTION

Traditional main-chain mesogen–non-mesogen liquid crystalline polymers are polymers in which flexible spacers alternate with mesogenic groups. The mesogenic groups are linearly substituted aromatic or cycloaliphatic rings further connected by small rigid units. The flexible spacers are usually repeating units with low barriers to rotation, such as a group of methylene units or aliphatic ethers. Typical examples of this type of liquid crystalline polymer are the poly(azomathine ether)s which we studied recently[1,2]. In contrast to mesogenic groups where the linearity and rigidity of the molecules is permanently set by the chemical structure, there is another class of mesogens where the rod-like character is realized through conformational isomerism and maintained only as long as the dynamic equilibrium between different conformers is frozen[3,4]. We have called this latter case a liquid crystalline polymer involving rod-like mesogenic groups based on conformational isomerism.

This idea was first realized in low molecular mass liquid crystals where ester groups were replaced by methyleneoxy groups within the structure of mesogenic groups[5–14]. Methyleneoxy units were successful in stabilizing the mesophase, particularly when they were used to interconnect two cycloaliphatic units or an aromatic and a cycloaliphatic unit. Low molecular mass liquid crystals containing a methyleneoxy unit in between two aromatic groups were also reported[9,14].

To synthesize these liquid crystalline polymers, one can introduce flexible interconnecting units, such as ethylene or methyleneoxy, to replace the more rigid interconnecting units in a mesogenic group. In this paper, we focus on one thermotropic polyether involving the rod-like mesogenic groups based on conformational isomerism, which was synthesized through 1-(4-hydroxyphenyl)-2-(2-methyl-4-hydroxyphenyl)ethane and α,ω-dibromopentane. This polymer has been designated MBPE-5 where 5 is the number of methylene units in the flexible spacers. The chemical structure of this polyether is:

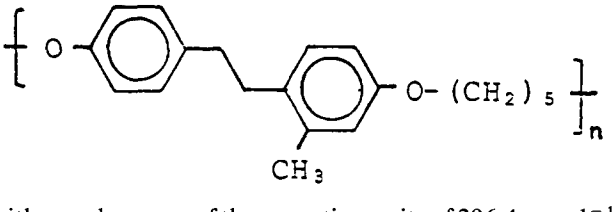

with a molar mass of the repeating units of 296.4 g mol^{-1}.

This paper presents the results of detailed investigations into the temperature- and time-dependent phase transition behaviour of MBPE-5. A liquid crystalline phase has been recognized in this polyether, and it is monotropic. Crystals with two different metastabilities can be identified. They have shown different crystalline morphologies. MBPE-5 is a first example of a whole series of MBPE-*m* where $m = 4$–12. We have chosen MBPE-5 simply because it shows the most complicated phase transition behaviour. The whole series of MBPE-*m* will be reported in our subsequent papers to establish relationships between structure and phase behaviour.

* To whom correspondence should be addressed

0032-3861/91/071284-09

EXPERIMENTAL

Materials. The synthesis of MBPE polymers has been published elsewhere[3,4]. The MBPE-5 studied here has been characterized via gel permeation chromatography (g.p.c.). Its number-average molecular mass is 19000 g mol^{-1} with a polydispersity of 1.9.

Polarized light microscopy (PLM). Optical microscopy under polarized light was performed on a Nikon Labophot-pol with a Mettler PF-52 hot stage. The hot stage temperature was calibrated with sharp melting point standards. The samples were prepared between two glass slides by heating above their melting temperature, and holding for 2 min. The samples were then cooled to predetermined temperatures quickly. Isothermal experiments were thus carried out. Photographs of the observed morphology were taken with a 35 mm camera.

Differential scanning calorimetry (d.s.c.). Thermal measurements were performed on both a Dupont 9900 thermal analyser and a Perkin–Elmer DSC2. Both were calibrated by following our standard procedures on temperature, heat flow and heat capacity measurements. All the samples were run under dry nitrogen atmosphere. Typical sample weights are between 6 mg and 12 mg for the heat capacity measurements.

Non-isothermal and isothermal experiments were carried out via d.s.c. The samples were heated to about 20 K above the melting temperature (410 K, see below) and held there for 2 min. They were then cooled down to 230 K at different cooling rates, or quickly quenched to predetermined isothermal temperatures (T_c) and crystallized for pre-fixed times (t_c).

Wide angle X-ray diffraction (WAXD). The WAXD experiments were carried out with a Rigaku X-ray generator. The point-focused beam was monochromatized with a graphite crystal to assure to Cu Kα radiation. X-ray powder diffraction diagrams were recorded on a diffractometer. A temperature controller was added on to the X-ray apparatus for thermal measurements. The precision of the controller was ±0.5 K in the temperature range studied. Programmed heating and cooling can be performed under control. Non-isothermal and isothermal experiments were carried out parallel to the d.s.c. experimental conditions in order to obtain comparative results.

RESULTS

Transition behaviour in d.s.c. measurements

Figure 1 shows a set of d.s.c. heating curves (heat capacity measurements) of the liquid-nitrogen quenched MBPE-5 samples from the melt (410 K) at different heating rates. Starting from the low temperature side, in the trace for the sample heated at 10 K min^{-1}, one can find a small glass transition-like behaviour at 242 K*. A bigger glass transition occurs at $T_g = 291$ K with $\Delta C_p = 125$ J K^{-1} mol^{-1} (extrapolated by both solid and liquid heat capacities of MBPE-5). An exothermic peak at about 303 K (peak temperature) immediately follows the glass transition. This process starts before the end of glass transition, as shown in *Figure 1*, since the ΔC_p measured is only about 100 J K^{-1} mol^{-1}. An endothermic peak can be observed at about 316 K, but again, it seems to overlap its neighbouring processes. The heats of transitions for those two processes are apparently rather small (*Table 1*, see below). At 322 K, a major exothermic peak appears, followed by a major endothermic peak at 350 K. After this endothermic process, an exothermic process follows very closely (about 355 K) indicating another overlap of two processes. Finally, a multiple peak endothermic process can be identified above 370 K. The transition behaviour is thus very complicated in this polyether as shown in *Figure 1*. Correct identification of the heat of transition in each process is the first step of our analyses. Assuming that we can bypass all the transitions during quenching, the basic understanding is that if there is no overlapping of two transition processes with opposite thermal effects, the heat of transition of the exothermic peak should be the same as that of the corresponding endothermic peak. Following this rule, we can separate the heats of transitions contributed by each process starting from the high temperature side, and determine the overlapped portions in each transition. The data are listed in *Table 1*. Basically, there are three pairs of transitions at the heating rate of 10 K min^{-1}, one occurs in the low temperature region below about 320 K, characterized by a heat of transition of 3–5 kJ mol^{-1}; one appears in the intermediate temperature region between about 320 K and 345 K characterized by a heat of transition of around 5.5–6 kJ mol^{-1} (low-temperature crystal, see below); and one is in the high temperature region above 345 K characterized by a heat of transition of around 2.5 kJ mol^{-1} (high-temperature crystal, see below).

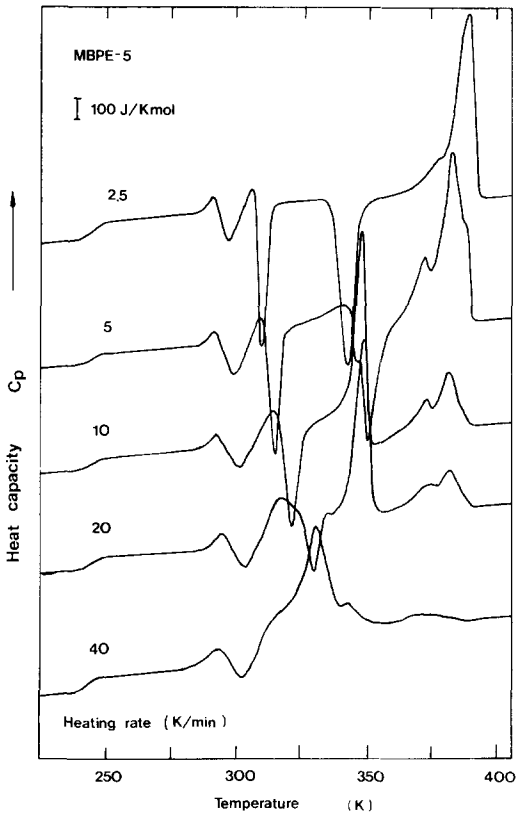

Figure 1 Set of d.s.c. heating curves of the liquid-nitrogen quenched MBPE-5 samples at different heating rates

* This low temperature glass transition-like behaviour is commonly observed in this series of polyethers which were quenched to liquid nitrogen before successive heating. This behaviour only appears in the quenched samples and will be discussed in our next publication

Table 1 Estimated transition temperature and heats of transition contributed by each process for quenched MBPE-5 at the different heating rates in *Figure 1*[a]

Heating rate (K min^{-1})	Heats of transition (kJ mol^{-1}) at different transition temperature regions					
	303 K	303–316 K	316–322 K	322–345 K	345–355 K	355–400 K
2.5[b]	−5.30 (−1.98)	3.33 (0.01)	−5.50 (−2.18)	6.50 (0.00)	−13.5 (−7.0)	13.5
5[b]	−5.15 (−1.88)	3.29 (0.22)	−6.05 (−2.98)	6.55 (0.46)	−10.5 (−4.41)	10.5
10[b]	−4.34 (−1.64)	3.24 (0.54)	−5.72 (−3.02)	5.92 (4.70)	−2.53 (−1.31)	2.53
20	−3.81 (−1.61)	3.15 (0.95)	−3.98 (−1.78)	3.98 (3.10)	−1.38 (−0.50)	1.38
40	−3.12 (−1.41)		3.12 (3.12)		−0.16 (−0.16)	0.16

[a]The values in parentheses are the observed data from the d.s.c. measurements, and the values out of parentheses are the estimated data without overlapping with neighbouring processes (see text)
[b]The samples heated at a heating rate slower than 10 K min^{-1} leads to the crystallization of the low-temperature crystal form during the transition process at around 303 K. At 2.5 K min^{-1}, it is approximately 1.0 kJ mol^{-1}; at 5 K min^{-1}, 0.5 kJ mol^{-1}; and at 10 K min^{-1}, 0.2 kJ mol^{-1}

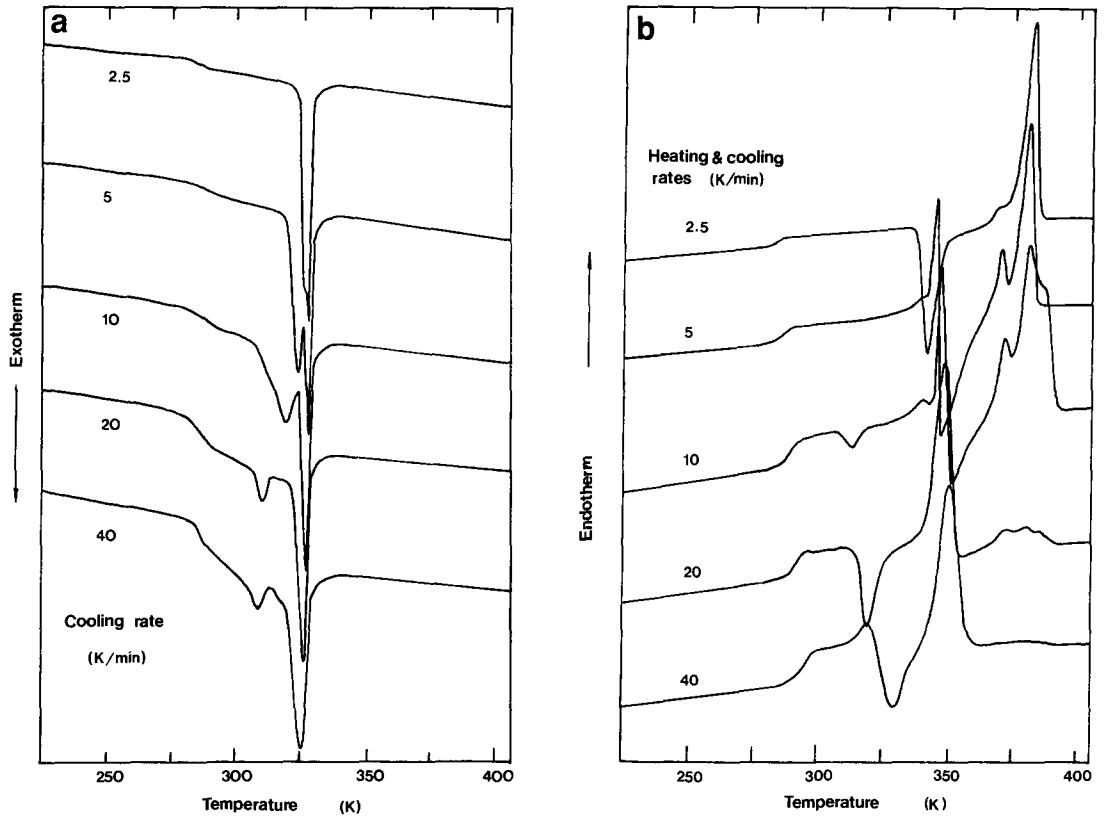

Figure 2 (a) Set of d.s.c. cooling curves of the MBPE-5 samples from the melt at different cooling rates. (b) Set of successive d.s.c. heating curves of the MBPE-5 samples cooled from the melt as shown in (a). The heating rate is the same as the preceding cooling rate for each case

Different heating rates may lead to the change of these three transitions. *Figure 1* shows that in the heating rate range studied the transitions in the low temperature region cannot be bypassed even at 40 K min^{-1}, and remnants of the two crystal formations in the intermediate and high temperature regions remain. Nevertheless, among the transitions they are more overlapped. The transition in the intermediate temperature region is less dependent on heating rate, although a minor decrease of the heat of transition with increasing heating rate can also be seen (*Table 1*). Following the rule proposed before, detailed data at different heating rates are also listed in *Table 1*.

When samples are cooled from the melt to 230 K at different cooling rates via d.s.c., exothermic peaks are expected, as shown in *Figure 2a*. For the sample cooled at 20 K min^{-1}, for example, two exothermic peaks can be observed at 326 and 309 K with heats of transitions of −3.25 and −1.32 kJ mol^{-1}, respectively. With decreasing cooling rate, the low-temperature exothermic peak temperature shifts towards the high temperature side faster than the high one. For example, at the cooling rate of 10 K min^{-1}, peaks appear at 327 and 318 K; and at 2.5 K min^{-1}, at 328 and 326 K, only two degrees apart. If the cooling rate is slow enough, one may expect that only the low-temperature transition is allowed as soon as it shifts to a temperature which merges with the high-temperature exothermic peak. The total heat of transitions for these two exothermic peaks also increases with decreasing cooling rate, namely from −4.11 kJ mol^{-1} at 40 K min^{-1} to −6.57 kJ mol^{-1} at 2.5 K min^{-1}. At a cooling rate slower than 5 K min^{-1}, the total heat of transitions is essentially unchanged (−6.57 kJ mol^{-1}). Interestingly enough, the heat of transition contributed

by the low-temperature exothermic peak increases with decreasing cooling rate. For example, at 40 K min^{-1}, the heat of transition of the low exothermic peak is -0.86 kJ mol^{-1}, and it increases to -3.30 kJ mol^{-1} at 2.5 K min^{-1}. Nevertheless, the heat of transition of the high-temperature exothermic peak is unchanged in the whole cooling rate range studied, and it keeps a constant value of -3.3 kJ mol^{-1}. The detailed data are listed in *Table 2*.

Figure 2b shows the heating curves for samples cooled and heated successively at the same rate. The exothermic transition in the intermediate temperature region (around 320 K, see *Table 2*) increases with increasing heating rate (compare the heating curve at 40 K min^{-1} with that at 10 K min^{-1}). The transition in the high temperature region appears to be less developed at a faster heating rate since less time is available to allow the molecules to crystallize. The transitions in the low temperature region, shown in *Figure 1*, cannot be seen during the heating, indicating that these crystals formed during the preceding cooling. All transition parameters (temperatures and heats of transition) are given in *Table 2*.

Phase behaviour in WAXD measurements

Figure 3 represents the WAXD patterns at different temperatures during heating of 5 K min^{-1} for the melt-quenched MBPE-5 samples (in liquid nitrogen). The immediate WAXD scanning for the quenched sample shows amorphous features. The diffraction peak is quite diffused with a maximum of about $2\theta = 19.7°$, indicating a spacing of 4.51 Å which is characteristic of an average distance between two neighbouring chain molecules in the amorphous state. At 303.2 K, a small but distinguishable diffraction peak starts to appear at $2\theta = 22.7°$ (d-spacing of 3.92 Å). This peak intensity slightly increases up to 323.2 K before other diffraction peaks become evident. At 333.2 K, three diffraction peaks at $2\theta = 16.4$, 19.7 and 23.4° (corresponding d-spacings of 5.40, 4.51 and 3.80 Å, respectively) appear. Above $T_c = 343.2$ K, an additional six diffraction peaks can be

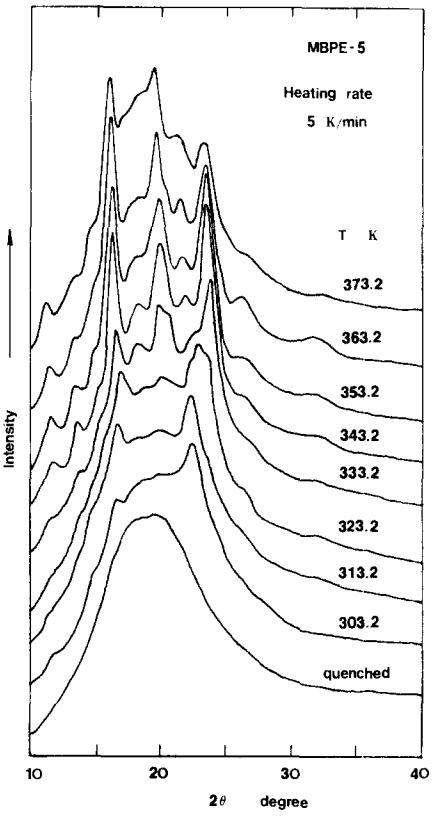

Figure 3 Set of WAXD curves of the liquid-nitrogen quenched MBPE-5 samples heated to 373.2 K at a heating rate of 5 K min^{-1}

Table 2 Estimated transition temperatures and heats of transition contributed by each process for MBPE-5 at the different cooling and heating rates in *Figure 2*[a]

Cooling from the isotropic melt

Cooling rate (K min^{-1})	Transition temperatures (K) and heats of transition (kJ mol^{-1})			
	T_i	ΔH_i	T_c	ΔH_c
40	325	−3.25	308	−0.86
20	326	−3.25	309	−1.32
10	327	−3.25	318	−2.86
5	328	−3.26	324	−3.20
2.5	328	−3.27	326	−3.30

Heating from 230 K after the samples cooled to 230 K at the same rates

Heating rate (K min^{-1})	Heats of transition (kJ mol^{-1}) at different transition temperature regions				
	315–320 K	320–335 K	335–355 K	355–365 K	365–400 K
40	2.93 (1.01)	−4.53 (−3.15)	5.39		0.21
20	1.93 (0.19)	−4.70 (−2.96)	6.02 (5.17)	−1.48 (−0.63)	1.48
10[b]	0.39 (0.10)	−0.66 (−0.37)	6.34 (1.84)	−6.49 (−1.48)	7.31
5[b]			5.46 (2.68)	−7.52 (−4.74)	8.52
2.5[b]			5.07 (0.61)	−10.0 (−5.54)	11.20

[a]The values in parentheses are the observed data from the d.s.c. measurements, and the values out of parentheses are the estimated data without overlapping with neighbouring processes

[b]The samples cooled from the isotropic melt at a cooling rate slower than the low-temperature crystal form, and this form is subsequently annealed to the high-temperature crystal form. At 10 K min^{-1}, it is approximately 0.82 kJ mol^{-1}; at 5 K min^{-1}, 1 kJ mol^{-1}; and at 2.5 K min^{-1}, 1.2 kJ mol^{-1}

observed; and they are $2\theta = 11.4$, 13.4, 15.1, 21.6, 26.3 and 31.4° (corresponding d-spacings of 7.76, 6.61, 5.87, 3.39 and 2.85 Å, respectively). They are representative of a crystal structure. The diffraction peak at $2\theta = 22.7°$ vanishes above $T_c = 333.2$ K. Further increasing the temperature leads to an increase of sharpness of the diffraction peaks and intensities, but the 2θ values are essentially unchanged. It should be also noted that the

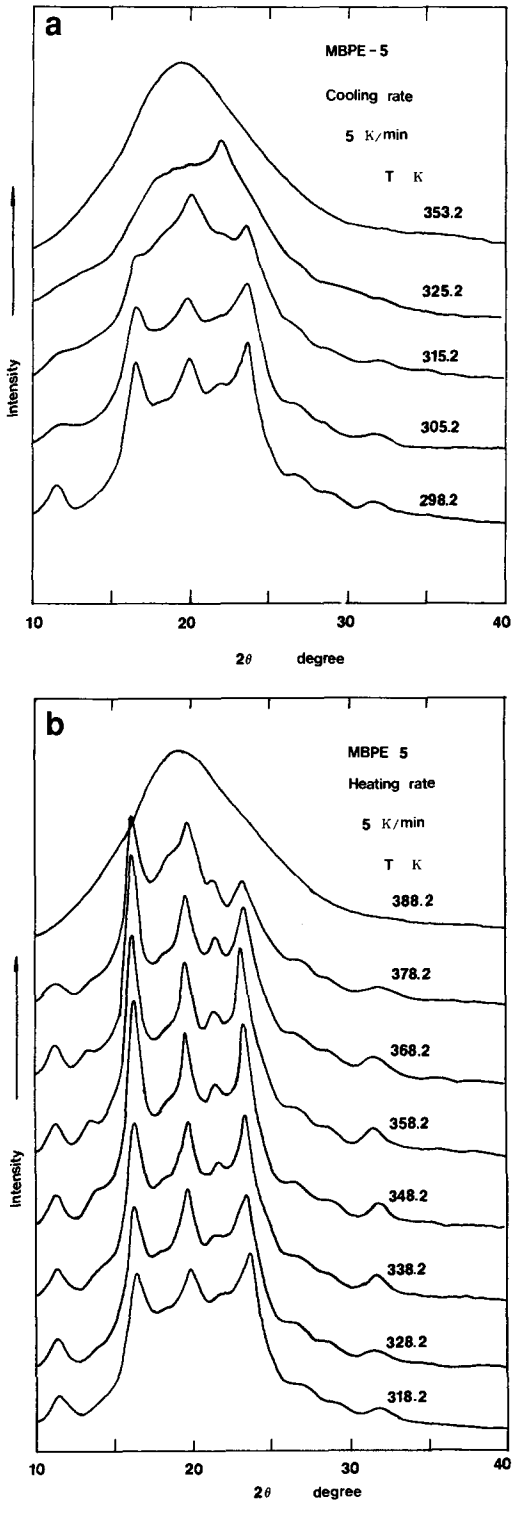

Figure 4 (a) Set of WAXD curves of the MBPE-5 samples cooled from the melt at a cooling rate of 5 K min^{-1}. (b) Set of successive WAXD curves of the MBPE-5 samples heated from room temperature to 388.2 K at a heating rate of 5 K min^{-1}. (The samples were cooled as shown in *Figure 4a* before heating.)

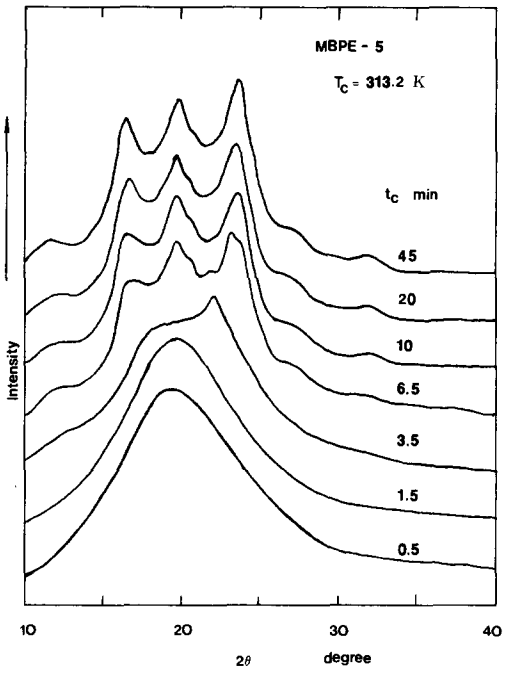

Figure 5 Set of WAXD curves of the MBPE-5 samples isothermally crystallized at 313.2 K from the melt at different times

absolute values of the increasing intensities for each diffraction peak are different. After the temperature reaches 353.2 K, the intensities start dropping, revealing the beginning of the crystal melting. But again, the diffraction peak with $2\theta = 23.4°$ decreases faster than those with $2\theta = 16.4$ and 19.7°.

Figure 4a shows a set of WAXD patterns for the MBPE-5 sample during cooling at 5 K min^{-1} from its isotropic melt. It is evident that above about 330.2 K, only an amorphous halo can be observed. The maximum of 2θ in this halo shifts from 18.9° at 383.2 K to 19.6° at 330.2 K. As soon as the temperature reaches 325 K, one small, but distinguishable diffraction peak at $2\theta = 22.7°$ (d-spacing of 3.92 Å) appears. On further decreasing the temperature, other diffraction peaks become clear and indicate that crystallization has taken place. *Figure 4b* is the WAXD results for the sample heated at 5 K min^{-1} from 298.2 K immediately after it was cooled down from the melt, as shown in *Figure 4a*. The WAXD results reveal that the crystal developed during the period prior to cooling is kept up to about 348.2 K. Further increasing the temperature leads to a decrease of absolute intensities, in particular at $2\theta = 23.4°$, similar to the case indicated previously in *Figure 3*.

Figure 5 shows an isothermal crystallization experiment at $T_c = 313.2$ K with the WAXD results at different crystallization times. It is clear that at $t_c = 3.5$ min, the sample undergoes a transition from its isotropic melt to a phase with a diffraction peak at $2\theta = 22.7°$ (corresponding d-space is 3.92 Å). After that time, other diffraction peaks gradually appear, with increases of the sharpness and intensities of the peaks, indicating a crystallization process.

Morphology observed in PLM experiments

Figures 6, 7 and *8* show the morphology of the MBPE-5 crystallized at different temperatures and times. *Figure 6* shows clearly a liquid crystalline pattern with schlieren texture from isothermal crystallization at 330 K.

If the cover slide is sheared after this pattern has formed, the flow nature can be observed within about 5 min (compared with the WAXD results in *Figure 5*). After that time, the shear stress needed becomes increasingly high. Finally, the texture of the samples breaks, indicating that the samples have solidified (crystallized), even though the liquid crystalline pattern is still essentially unchanged.

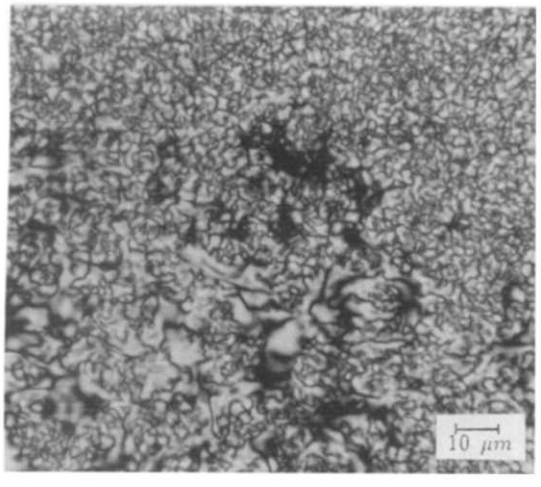

Figure 6 Liquid crystalline pattern with schlieren texture of the MBPE-5 samples isothermally crystallized at 330 K for 10 min

Crystallizing at 340 K leads to interesting behaviour, as shown in *Figure 7*. The type I spherulitic texture forms predominantly in a short period of time (up to about 1 h). Growth of another type (II) of spherulite can then be observed which shows brighter birefringence with clearer banding patterns which appear later, but grow faster. This type of pattern indicates that at the location of the rings the molecular axis is parallel to the illumination[15]. The extinction cross is barely seen in this type of spherulite (*Figure 7d*). A successive heating in PLM at 10 K min^{-1} indicates that the type II spherulites melt at 370 K, and type I spherulites, at 378 K, respectively.

It is evident that the sample crystallized at high temperature (360 K), as shown in *Figure 8*, and grows spherulites (type I) which exhibit extinction crosses with banding. As is well-known, such banding is common in polymer spherulites and is attributable to a twisting of crystallographic orientation about radii that apparently reflect cooperative twisting of radiating lamellar crystals about their axes of fastest growth[16].

A special observation in the MBPE-5 samples is that their nucleation during crystallization seems to be a thermal type, namely, the primary nuclei are created continuously with increasing time in the temperature region above 330 K. As a result, one cannot clearly divide two processes, nucleation and crystal growth, in the overall crystallization, unless the actual nucleation rate is known.

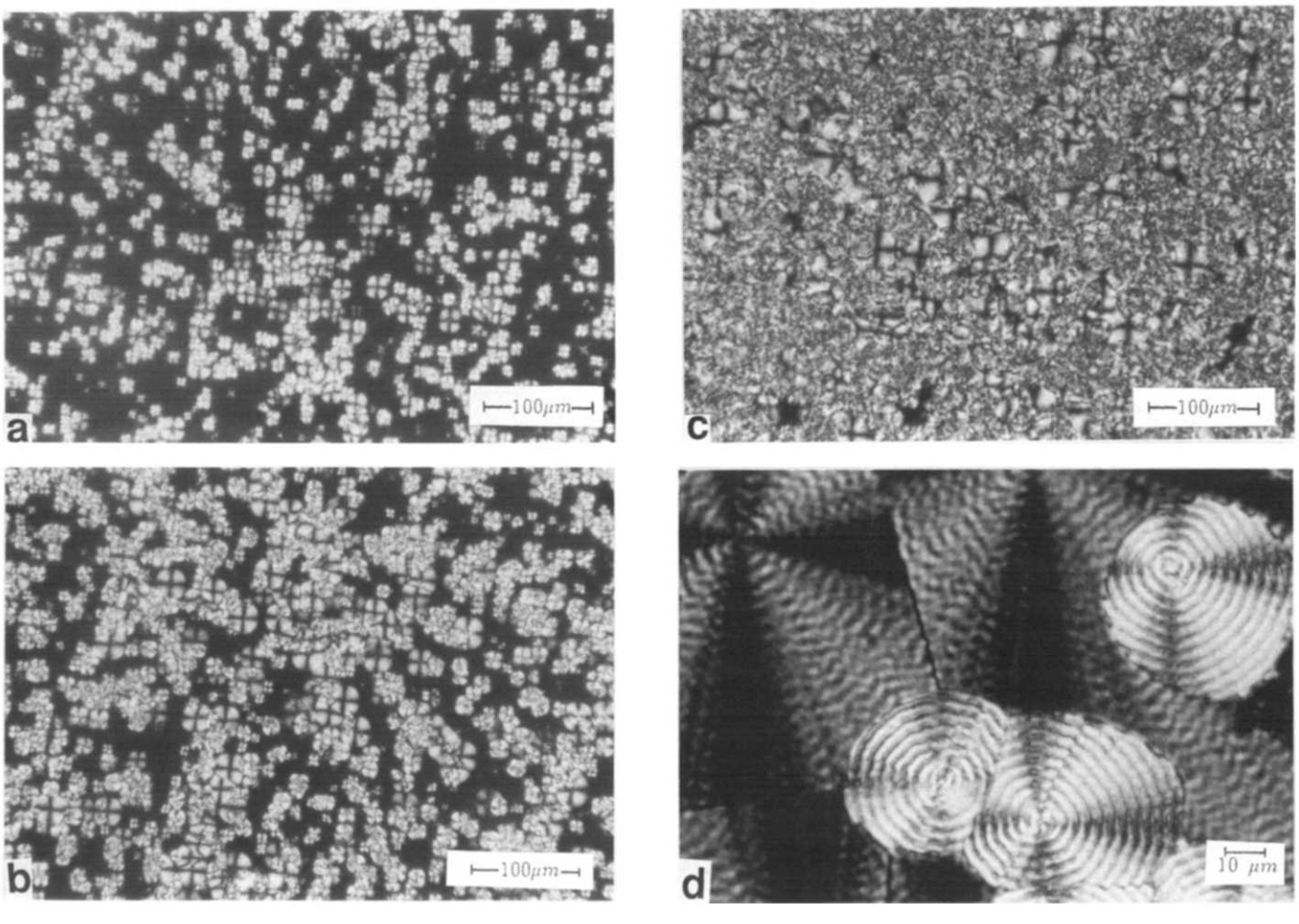

Figure 7 MBPE-5 samples crystallized at 340 K for (a) 60 min, (b) isothermal crystallization for 120 min, (c) isothermal crystallization for 255 min, (d) enlarged (c)

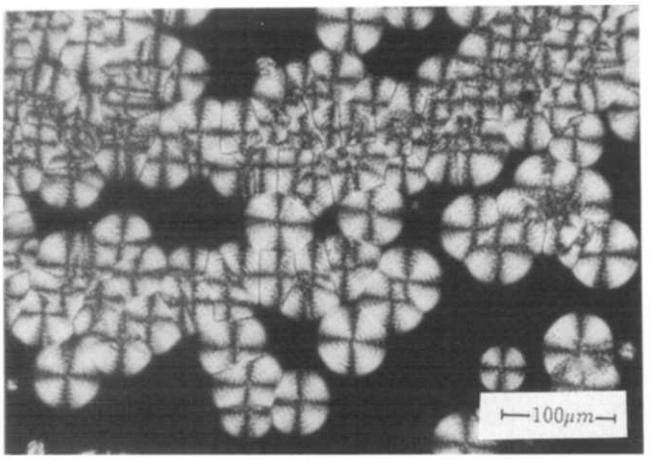

Figure 8 MBPE-5 samples crystallized at 360 K for 260 min

DISCUSSION

All of our experimental observations indicate that the MBPE-5 samples show complicated transition behaviour as well as their corresponding morphology. In this section, we try to focus on whether a liquid crystalline phase exists in the MBPE-5 samples, and if there is, what is its transition behaviour?

To identify a liquid crystalline phase, several experimental methods ought to be applied. From d.s.c. measurements, a thermotropic liquid crystalline transition can be commonly identified through the transition sequence of crystal/liquid crystal/isotropic melt[20]. It is well-known that enthalpy and entropy changes of the transition between a liquid crystalline and an isotropic phase is very small, and is usually less than 10% of the total enthalpy or entropy changes between a rigid crystal and its corresponding isotropic melt[20]. From a thermodynamic point of view, the relationship between Gibbs free energy and temperature for different phase transitions is illustrated in *Figure 9a*. It is clear that the transition temperature T_d from a rigid crystal to a liquid crystalline phase is lower than the isotropization, T_i, which is the transition from a liquid crystalline to an isotropic phase. However, in our case of the MBPE-5 samples, one cannot find an isotropization transition above the crystal melting of the high-temperature crystal in the bulk samples at 388 K. This indicates that if there is any liquid crystalline phase, its transition must occur below the crystal melting temperature. From our d.s.c. heating experiments of liquid-nitrogen quenched samples, one can find a transition just above the T_g (291 K), as shown in *Figure 1*, with a heat of the transition of about 3–4 kJ mol^{-1}, which is about one order of magnitude smaller than the heat of fusion during the crystal melting*. Furthermore, this transition is less heating-rate dependent during heating (*Figure 1*), and needs little supercooling during cooling (*Figure 2a*). Most importantly, the heat of this transition is constant (3.3 kJ mol^{-1}) at different cooling rates (*Figure 2a* and *Table 2*).

* Based on the two phase (crystallinity) model, we have found that the successive heating of the MBPE-5 sample which was cooled at -10 K min^{-1} from its melt shows a ΔC_p of 83.3 kJ K^{-1} mol^{-1} with a Δh_f of 6.34 kJ mol^{-1}. Since the ΔC_p of total amorphous MBPE-5 is 125 J K^{-1} mol^{-1}, the equilibrium heat of transition can be roughly estimated to be 19 kJ mol^{-1}

Our PLM observations reveal that a liquid crystal tern with schlieren texture can be observed when the ıples were quenched from the melt to below 330 K isothermal experiments (*Figure 6*). This texture is akin

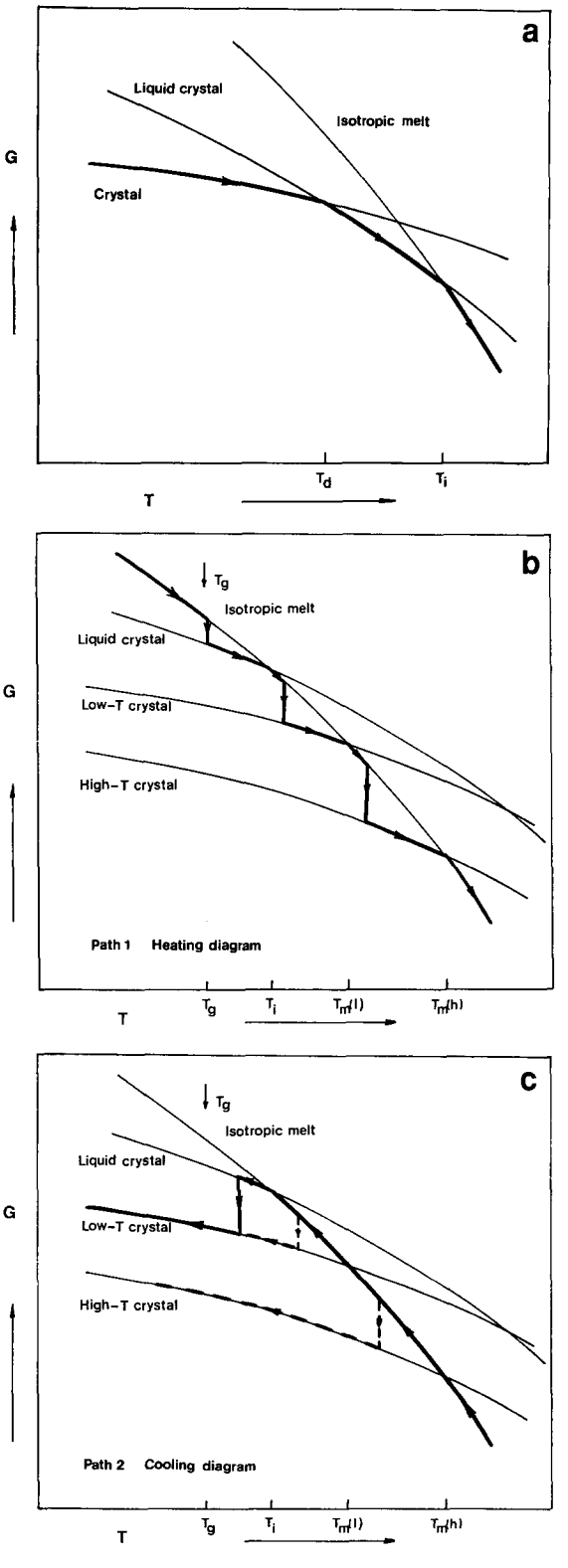

Figure 9 (a) Relationship between Gibbs free energy of each state and temperature for a normal case. (b) Relationship between Gibbs free energy of each state and temperature of the liquid-nitrogen quenched MBPE-5 samples with a monotropic phase during heating (path 1). (c) Relationship between Gibbs free energy of each state and temperature of the MBPE-5 samples during cooling from the isotropic melt (path 2, the broken lines represent the path of different cooling rates)

to those reported for a variety of liquid crystalline polymers[21,22]. Furthermore, in the initial stage of the experiments (up to a few minutes) the samples can be sheared easily, indicating a flow nature.

Finally, during heating of the quenched MBPE-5 sample (*Figure 3*), cooling from the isotropic melt (*Figure 4a*) or isothermal experiment at 313.2 K (*Figure 5*), a rather disordered state is always indicated by our WAXD measurements with a diffraction peak at $2\theta = 22.7°$. This peak does not exist in the later crystalline state. In fact, we have determined the crystal unit cell of this sample, and it is triclinic with $a = 12.94$ Å, $b = 9.538$ Å, $c = 33.74$ Å, $\alpha = 43.4°$, $\beta = 109.2°$ and $\gamma = 104.7°$. This 2θ diffraction peak does not correspond to any crystalline plane in this triclinic lattice structure (detailed results will be published elsewhere). Therefore, we conclude that based on our observations of three independent methods, a liquid crystalline phase does exist in the MBPE-5 samples. This transition behaviour is however, monotropic[25,26].

A phenomenological definition of such a monotropic phase is a system which only exhibits a stable liquid crystalline phase when cooled below its clearing temperature. From a thermodynamic point of view, *Figure 9b* illustrates this kind of phenomenon via a plot of the change of Gibbs free energy with respect to temperature, similar to *Figure 9a*. In this case the crystal melting temperature, T_m, is higher than the transition temperature, T_i, from the liquid crystalline to isotropic phases; namely, the curvature of the liquid crystalline state, $\partial^2 G/\partial T^2 = -C_p/T$, is in between those of liquid and crystalline states. In *Figure 9*, we have drawn two crystal Gibbs free energy curves with respect to temperature since two different metastable crystals exist in the MBPE-5 samples. To explain our d.s.c. heating and cooling curves (*Figures 1* and *2a*) via *Figures 9b* and *c*, we must further consider the kinetic effects of the phase transitions. As a first example, one may follow the heating curve of the liquid-nitrogen quenched samples (*Figure 9b*). Assuming we can bypass all the exothermic processes during quenching, Gibbs free energy of the sample starts at the liquid line. As soon as the sample passes its T_g, the molecules gain enough mobility to form the liquid crystalline phase in order to decrease the Gibbs free energy, which is an exothermic process. Since the transition temperature to its isotropic melt, T_i, is close to T_g, the liquid crystalline phase starts isotropolizing (an endothermic process) right after this exothermic process. With increasing temperature, crystallization of the low-temperature crystal further decreases the Gibbs free energy. After the Gibbs free energy of the low-temperature crystal reaches the intersection point with that of the isotropic melt, the low-temperature crystal melts, indicating an endothermic process. However, the path cannot follow this liquid line too far since the crystallization of the high-temperature crystal occurs due to the thermodynamic driving force. This high-temperature crystal melts at T_m (h) as soon as the Gibbs free energy of high-temperature crystal reaches that of the isotropic melt liquid line. The kinetic effects are represented by the temperatures where the transitions occur, which may not be in the equilibrium conditions.

The cooling curves (*Figure 2a*) may involve further consideration of the kinetic effects, as shown in *Figure 9c*. Starting from its isotropic melt phase, if the cooling rate is fast enough, we may bypass both T_m(h) and T_m(l) due to crystal nucleation which usually needs supercooling to overcome nucleation barriers[27,28]. Until the Gibbs free energy line of the supercooled isotropic melt reaches T_i, an exothermic process occurs, and the liquid crystalline phase forms since this transition needs little supercooling, as shown in *Figure 2a* and *Table 2*. Nevertheless, the low-temperature crystal still tries to develop in order to further decrease the Gibbs free energy. Such a crystallization process can be observed in *Figure 9c* before the sample reaches T_g. As shown in *Figure 2a*, it is clear that with increasing the cooling rate, the low-temperature exothermic peak, which is characterized as the growth of the low-temperature crystal, quickly shifts to lower temperature, and its heat of transition decreases (at a cooling rate of 40 K min^{-1}, this peak temperature does not show a further shift to lower temperature. This is possibly due to the influence of its T_g). Another limitation is if the cooling rate is slow enough, and we cannot bypass the crystallization process, the liquid crystalline phase is thus forbidden to appear due to thermodynamic reasons (*Figure 9c*). As soon as the final state during the cooling ends in the crystalline phase, the liquid crystalline phase cannot be seen in the successive heating as shown in *Figure 2b*.

Furthermore, the transition from the isotropic melt to the low-temperature crystal is in the temperature region between its glass transition and 330 K (*Figure 1*). However, our PLM observations indicate a typical liquid crystalline pattern with schlieren texture (*Figure 6*), revealing that to crystallize the low-temperature crystal one cannot bypass the liquid crystalline phase in the low isothermal temperature region. In fact, the flow nature of the MBPE-5 samples in the initial stage of their crystallization is an additional piece of evidence for this conclusion. By increasing the isothermal time, crystallization occurs (*Figure 5*), but its morphology observed via PLM does not change, indicating that the crystallization process is undertaken on a finer, microscopic scale (say, in the order of 10–100 nm). We may speculate that the crystals formed via its parent liquid crystalline phase may preserve the local orientation order of that state as proposed by Wendorff *et al.*[29,30] and Blumstein *et al.*[31]. Of special interest is the growth of two types of spherulites in a narrow temperature region between 330 K and 345 K. The type I spherulites are obviously attributed to the high-temperature crystal, which corresponds to the melting temperature of 378 K. The type II spherulites are however, less ordered, which can be judged by a lower melting temperature at 370 K. The quicker growth of the type II spherulites may largely hamper the further growth of type I spherulites. The detailed mechanism may involve non-negligible fractions of crystal nuclei, or change of growth rate during crystallization in addition to low dimensional crystal growth[19,32]. The explanation of the formation of these two types of spherulites is not well understood; they might be attributed to the two different metastable crystals. Further investigation is currently being undertaken.

The key problem still remains: why this polyether, MBPE-5, exhibits such an unusual transition behaviour? The quantitative answer is still largely uncertain. Qualitatively, this behaviour must be related to its rod-like mesogenic groups based on conformational isomerism. When the methylene groups between two phenylene groups keep the *trans* conformation, the whole mesogenic group can still be thought to be rod-like, and may show

liquid crystalline behaviour. However, this kind of *trans* conformation may reach an equilibrium compared with the *cis* conformation. As a result, only part of this polymer is in the liquid crystalline state. Furthermore, this liquid crystalline phase is less stable, and therefore, its Gibbs free energy is higher compared with conventional liquid crystalline phases. As shown in *Figures 9b* and *c*, a stable liquid crystal to isotropic melt transition does not occur above the crystal melting temperature. Such liquid crystalline behaviour should strongly depend upon an external force field. Indeed, our preliminary study has indicated such dependence[33]. A detailed description of the transition behaviour, ordering and molecular motion also relies on the further structure characterization from WAXD, rheo-optical and solid-state n.m.r. measurements.

CONCLUSIONS

The MBPE-5 thermotropic polyether consists of rod-like mesogenic groups based on conformational isomerism of methylene flexible spacers and shows complicated transition behaviour. Several conclusions can be drawn from our experimental observations:

1. the MBPE-5 sample shows a liquid crystalline phase which is monotropic;
2. two different metastable crystals can be identified: a low- and a high-temperature crystal in the MBPE-5 samples;
3. above the isothermal temperature 345 K, the high-temperature crystal can grow from its isotropic melt, forming type I spherulites with clear distinction cross and banding pattern;
4. the formation of the low-temperature crystal can be through its parent liquid crystalline phase. Further crystallization does not change the liquid crystalline pattern (schlieren texture) but flow behaviour, indicating that this process occurs on a smaller scale;
5. between 330 K and 345 K, two types of the spherulites grow. They might be related to the two different metastable crystals.

ACKNOWLEDGEMENTS

This work is partially supported by Exxon Educational Foundation. Mr P. Giusti's help with optical microscopy measurements is acknowledged.

REFERENCES

1 Cheng, S. Z. D., Janimak, J. J., Sridhar, K. and Harris, F. W. *Polymer* 1989, **30**, 494
2 Cheng, S. Z. D., Janimak, J. J., Lipimski, T., Sridhar, K., Huang, X.-Y. and Harris, F. W. *Polymer* 1990, **31**, 1122
3 Percec, V. and Yourd, R. *Macromolecules* 1988,**21**, 3379
4 Percec, V. and Yourd, R. *Macromolecules* 1989, **22**, 524
5 Gray, G. W. and McDonnell, D. G. *Mol. Cryst. Liq. Cryst.* 1979, **53**, 147
6 Gray, G. W. *Mol. Cryst. Liq. Cryst.* 1981, **63**, 3
7 Osman, M. A. *Mol. Cryst. Liq. Cryst.* 1982, **72**, 291; **82**, 47; **82**, 295
8 Takatsu, H., Takeuchi, K. and Sato, H. *Mol. Cryst. Liq. Cryst.* 1984, **111**, 311
9 Carr, N. and Gray, G. W. *Mol. Cryst. Liq. Cryst.* 1985, **124**, 27
10 Kelly, S. M. and Schad, H. *Helv. Chim. Acta* 1985, **68**, 1444
11 Carr, N., Gray, G. W. and Kelly, S. M. *Mol. Cryst. Liq. Cryst.* 1985, **29**, 301
12 Abdullah, H. M., Gray, G. W. and Toyne, K. J. *Mol. Cryst. Liq. Cryst.* 1985, **124**, 105
13 Eidenschink, R. *Mol. Cryst. Liq. Cryst.* 1985, **123**, 57
14 Tinh, N. H., Gasparoux, H. C. and Destrade, C. *Mol. Cryst. Liq. Cryst.* 1985, **123**, 271
15 Bassett, D. C. 'Principles of Polymer Morphology', Cambridge University, Cambridge, 1981
16 Keith, H. D., Padden, F. J. Jr and Russell, T. P. *Macromolecules* 1989, **22**, 666
17 Cheng, S. Z. D. and Wunderlich, B. *Macromolecules* 1986, **19**, 1868; 1987, **20**, 1630; 1987, **20**, 2082; 1988, **21**, 789
18 Cheng, S. Z. D., Heberer, D. P., Lien, H.-S. and Harris, F. W. *J. Polym. Sci., Polym. Phys. Edn* 1990, **28**, 655
19 Cheng, S. Z. D. *Macromolecules* 1988, **21**, 2475
20 Wunderlich, B. and Grebowicz, J. *Adv. Polym. Sci.* 1984, **60/61**, 1
21 Demus, D. and Richter, L. 'Textures of Liquid Crystals', Verlag Chemie, Weihheim, 1978
22 Noel, C. in 'Recent Advances in Liquid Crystalline Polymers' (Ed. E. L. Chapoy), Elsevier Applied Science, New York, 1985
23 de Vries, A. *Mol. Cryst. Liq. Cryst.* 1970, **10**, 219; Wendorff, J. H. in 'Liquid Crystalline Orders in Polymers' (Ed. A. Blumstein), Academic Press, New York, 1978
24 Pollack, S. K., Shan, D. Y., Wang, Q., Stidham, H. D. and Hsu, S. L. *Macromolecules* 1989, **22**, 551
25 Barrall, E. W. in 'Liquid Crystals: The Fourth State of Matter' (Ed. F. D. Saeva), Marcel Dekker, New York, 1979
26 Zhou, Q.-F., Duan, X.-L. and Liu, Y.-L. *Macromolecules* 1986, **19**, 247
27 Mandelkern, L. 'Crystallization in Polymers', McGraw-Hill, New York, 1964
28 Wunderlich, B. 'Macromolecular Physics, Crystal Nucleation, Growth, Annealing', Vol. 2, Academic Press, New York, 1976
29 Bechtoldt, H., Wendorff, J. H. and Zimmerman, H. J. *Makromol. Chem.* 1987, **188**, 651
30 Wendorff, J. H. Frick, G. and Zimmerman, H. J. *Mol. Cryst. Liq. Cryst.* 1988, **157**, 455
31 Blumstein, R. B., Stickles, E. M., Gauthier, M., Blumstein, A. and Volino, F. *Macromolecules* 1984, **17**, 177
32 Cheng, S. Z. D. and Wunderlich, B. *Macromolecules* 1988, **21**, 3327
33 Unpublished data in our laboratory. For the MBPE-5 samples, a mesophase appears above the crystal melting temperature of 378 K under shearing. Therefore, the shearing lowers the Gibbs free energy line of the liquid crystal in *Figure 9b* to reach an intersection with that of the isotropic melt above the crystal melting temperature, $T_m(h)$